



Cite this: *Dalton Trans.*, 2015, **44**, 12326

Comparing a series of 8-quinolinolato complexes of aluminium, titanium and zinc as initiators for the ring-opening polymerization of *rac*-lactide†

Clare Bakewell,^a Giovanna Fateh-Iravani,^a Daniel W. Beh,^a Dominic Myers,^a Sittichoke Tabthong,^b Pimpa Hormnirun,^b Andrew J. P. White,^a Nicholas Long^{*a} and Charlotte K. Williams^{*a}

The preparation and characterization of a series of 8-hydroxyquinoline ligands and their complexes with Ti(IV), Al(III) and Zn(II) centres is presented. The complexes are characterized using NMR spectroscopy, elemental analysis and, in some cases, by single crystal X-ray diffraction experiments. The complexes are compared as initiators for the ring-opening polymerization of racemic-lactide; all the complexes show moderate/good rates and high levels of polymerization control. In the case of the titanium or aluminium complexes, moderate iso-selectivity is observed ($P_i = 0.75$), whereas in the case of the zinc complexes, moderate hetero-selectivity is observed ($P_s = 0.70$).

Received 15th January 2015,
Accepted 24th February 2015

DOI: 10.1039/c5dt00192g

www.rsc.org/dalton

Introduction

Lewis acidic metal alkoxide/amide complexes have become popular choices as the initiators in the ring-opening polymerization of lactones.¹ This is relevant because ROP can be used to prepare bio-derived and/or bio-compatible polyesters, such as polylactide which are proposed as sustainable alternatives to common petrochemicals.² Metal catalysed, or more precisely initiated, polymerizations are proposed to occur by a coordination-insertion mechanism whereby the Lewis acidic metal centre coordinates the lactide, activating it to attack by a metal bound alkoxide group. This attack leads to ring-opening and generation of a new metal alkoxide species. The selection of the initiator is important as it affects features such as the polymerization rate, the degree of polymerization control (end-groups/molecular weight, dispersity, facility to form block copolymers) and the stereocontrol. Initiators which are able to efficiently produce PLA, with stereocontrol are of interest as the different tacticities of PLA result in different performances, in particular in different thermal and mechanical properties.^{1a-d} Well-defined, *i.e.* ligated, metal complexes are frequently targeted as catalysts; they are particularly attractive as the ligand-metal interactions moderate and control the

catalysis. The application of earth-abundant metal centres is especially desirable as a means to reduce the cost and improve sustainability of the initiator selection. There is already a strong track record for use of some of the most earth-abundant metal centres including successful initiators of Al(III),³ Fe(III),⁴ Ca(II),⁵ Mg(II),^{5b,d,6} Na(I),⁷ K(I)^{7a,8} and Ti(IV).⁹ Despite these successes there is still a strong drive for new initiators particularly those able to exert high degrees of polymerization control, especially stereocontrol.

Results and discussion

Our approach was to prepare complexes of earth abundant elements using a series of easily synthesised and moderated ancillary ligands. The use of 8-hydroxyquinoline ligands is attractive as they are either commercially available or easily synthesised and, from the point of view of catalysis, offer a large range of different sites for substitution, most notably at positions R₁₋₃, which enable modifications of the steric and electronic features of the complexes.¹⁰ Some of us have previously reported Group 13 complexes of several 8-hydroxyquinoline ligands; these complexes are slow but iso-selective initiators in the polymerization of *rac*-lactide.^{10b} It was discovered that modifications to the R₁ and R₃ substituents led to increased iso-selectivity and polymerization activity, respectively.^{10b} Further, the (8-quinolinolato)gallium analogues were significantly faster initiators highlighting the importance of the metal centre in moderating catalysis.^{10a,b} It was, therefore, of interest to explore a wider range of 8-hydroxyquinoline

^aDepartment of Chemistry, Imperial College London, London SW7 2AZ, UK.
E-mail: c.k.williams@imperial.ac.uk, n.long@imperial.ac.uk

^bDepartment of Chemistry, Faculty of Science, Kasetsart University, Bangkok 10900, Thailand

† Electronic supplementary information (ESI) available. CCDC 1043547–1043549. For ESI and crystallographic data in CIF or other electronic format see DOI: 10.1039/c5dt00192g



complexes, using Al(III), Ti(IV) and Zn(II), to explore the effects on polymerization catalysis.

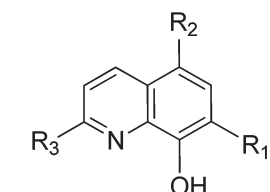
Pro-ligand syntheses

A series of 8-hydroxyquinoline pro-ligands were selected for the study; their structures are illustrated in Fig. 1. Pro-ligands A–D are either commercially available or were prepared by previously described literature procedures and all have methyl substituents at position R₃ and a range of different halides/H at positions R₁ and R₂.^{10b} Pro-ligand E was also prepared by a modified literature route (see ESI†) and differs from ligand D by having a larger phenyl substituent at position R₃.¹¹ Compounds F and G have phenyl and ethynyl ferrocene substituents at position R₁, with the other substituents being the same as ligand A. They were targeted to investigate the influence of aromatic substituents at the position *ortho*- to the phenolate moiety. Compounds F and G were prepared from the mixed halide pro-ligand B, *via* sequences of protection of the phenol group; followed by cross-coupling reactions with the iodo-

substituent (R₁) using Suzuki (for F) or Sonagashira (for G) methods; followed by deprotection of the phenol which enabled isolations in good overall yields (57% for F and 68% for G). The new pro-ligands E–G were fully characterised by NMR spectroscopy, mass spectrometry and the stoichiometry was confirmed by elemental analysis. Further details of the ligand syntheses are available in the ESI (Schemes S1 and 2†).

Complex syntheses

Aluminium complexes. We have previously reported bis(8-quinolinolato) aluminium ethyl complexes, [L₂AlEt] where L = ligands A–D.^{10b} The catalytic performance data are included for reference here and the complexes are labelled Al-A/B/C/D, respectively. New analogous bis(8-quinolinolato) aluminium ethyl complexes, Al-E, Al-F and Al-G, were synthesised by the reaction of two equivalents of the relevant 8-hydroxyquinoline pro-ligands, (E, F or G), with triethyl aluminium, in toluene at 298 K (Fig. 2). Compounds Al-E and Al-F were isolated as crystalline yellow (Al-E or Al-F) or orange (Al-G) solids (isolated yields: 71% Al-E; 34% Al-F; 63% Al-G). The new complexes were characterized using ¹H NMR spectroscopy, where signals assigned to protons on the ligands and those assigned to the aluminium coordinated ethyl group were observed. The ligand signals were typically observed at lower chemical shift compared to the pro-ligands, consistent with coordination to a Lewis acidic metal centre (Al). A triplet was observed at 0.21, 1.05 and 0.67 ppm, for Al-E/F/G, respectively, assigned to the methyl protons of the aluminium ethyl group. Two quartets were typically observed at 0.25–0.75 ppm due to the diastereotopic methylene protons on the same aluminium ethyl group. It is notable that the diastereotopic methylene protons of compound Al-E were observed at a considerably lower shift, –1.08 ppm, with the two quartets only being observable using a higher resolution 500 MHz NMR instrument. The observed signal multiplicity for the aluminium ethyl groups is in line with the characterization data for the previously reported complexes.^{10b} The purity of the new complexes Al (E–G) was confirmed by elemental analyses.



#	R ₁	R ₂	R ₃
A	Cl	Cl	Me
B	I	Cl	Me
C	Br	Br	Me
D	H	H	Me
E	H	H	Ph
F	Ph	Cl	Me
G	ethynyl ferrocene	Cl	Me

Fig. 1 The structures of a series of 8-hydroxyquinoline compounds A–G.

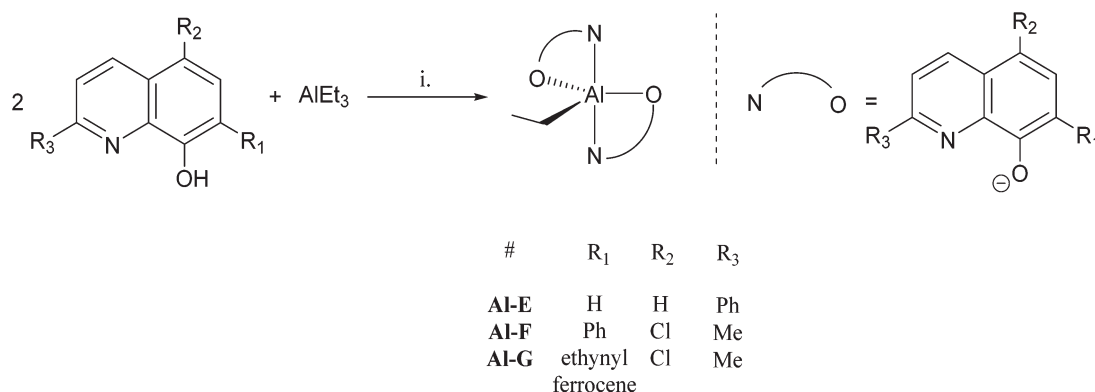


Fig. 2 General synthesis of initiators Al-E, F and G, numbering scheme included. Reagents and conditions: i. AlEt₃, toluene, 298 K, 12 h, Al-E (71%), Al-F (34%), Al-G (63%).



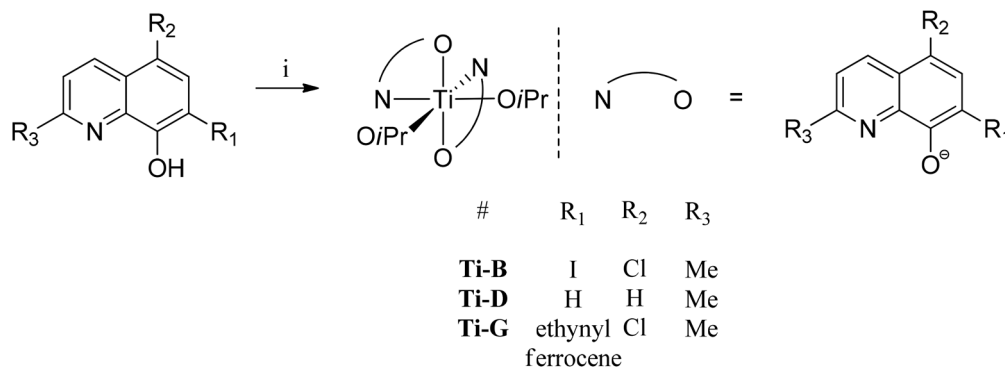


Fig. 3 General synthesis of initiators **Ti-B**, **D** and **G**, numbering scheme included. Reagents and conditions: i. $\text{Ti}(\text{OiPr})_4$, toluene, 298 K, 12 h, **Ti-B** (70%), **Ti-D** (43%), **Ti-G** (64%).

Titanium(IV) complexes. A series of three new bis(8-quinolinolato) bis(iso-propoxide) titanium(IV) complexes, $[\text{L}_2\text{Ti}(\text{OiPr})_2]$ were targeted, where **L** was selected based on a precedent for formation of high activity/selectivity aluminium catalysts as well as applying new pro-ligand **G** (aromatic R_1 substituent) (Fig. 3). Thus, compounds **Ti-B**, **Ti-D** and **Ti-G** were synthesised by reaction of one equivalent of titanium(IV) *tetrakis*(iso-propoxide) with two equivalents of ligands **B**, **D** and **G**, respectively, in toluene solution, at 298 K. The new complexes were isolated as yellow (**Ti-B** and **D**) or orange (**Ti-G**) solids in moderate to good yields (43–70%).

The new compounds were characterised by NMR spectroscopy and the purity was confirmed by elemental analysis. The characteristic peaks of the iso-propoxy alkoxide groups resonate as a septet (4.8–5.2 ppm) and a doublet of doublets (1.2–1.4 ppm), and integrate at a 1 : 1 ratio with the quinolate peaks confirming the proposed complex stoichiometry. Although X-ray crystal structures of the new titanium(IV) complexes were not obtained, the complexes are proposed to adopt distorted octahedral geometries with the N atoms, of the quinolate ligands, being in a *cis*-disposition to one another and the O-atoms being in *trans*-positions (see Fig. 3). Such a geometry is different to that observed for the pentacoordinate $\text{Al}(\text{III})$ complexes, but is in line with other X-ray crystal structures reported for closely related bis(8-quinolinolato) bis(iso-propoxide) complexes of titanium(IV).¹²

Zinc complexes. Although zinc is not as prevalent an element as Al or Ti, it is of interest to investigate its coordination chemistry with the 8-hydroxyquinoline ligands. This is because of the strong track record of zinc alkoxide initiators showing high rates and stereoselectivity. A series of (8-quinolinolato)zinc ethyl complexes, $[\text{LZnEt}]$ where **L** is ligand **A–E**, **G**, were prepared (Fig. 4). The 8-hydroxyquinoline pro-ligands (**A–E** and **G**) were reacted with an equimolar quantity of diethyl zinc, in toluene, at 298 K. During the course of the reaction a precipitate formed which, after stirring for 12 hours, was isolated by filtration to yield the zinc complexes as yellow (**Zn-A–E**) or orange (**Zn-F**) solids in good yields (55–78%). The new compounds were characterised by NMR spectroscopy and the purity was confirmed by elemental analysis. The ^1H NMR

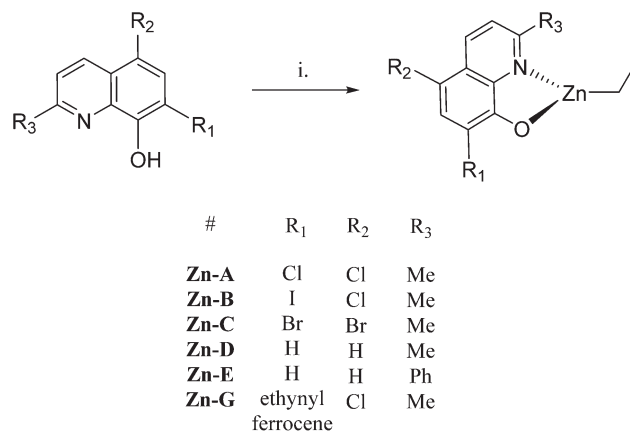


Fig. 4 General synthesis of initiators **Zn-A**, **B**, **C**, **E** and **G**, numbering scheme included. Reagents and conditions: i. ZnEt_2 , toluene, 298 K, 12 h, **Zn-A** (78%), **Zn-B** (70%), **Zn-C** (56%), **Zn-D** (67%), **Zn-E** (70%), **Zn-G** (60%).

spectra showed the characteristic shift to lower chemical shifts in the ligand signals compared to those of the pro-ligands. The zinc ethyl groups showed a quartet, at ~0.4 ppm, due to the methylene protons, and a triplet, at 1.2–1.3 ppm, assigned to the methyl protons.

Single crystal X-ray diffraction experiments revealed that compound **Zn-A** exists as a dimer in the solid state, *vide infra*. On the basis of this finding, it is tentatively assumed that other complexes with sterically hindered substituents at sites R_1 and R_2 are also dimeric in the solid state, *i.e.* complexes **Zn-(A–C)** and **Zn-G**. Consistent with this proposal is the finding that these complexes (**Zn-(A–C)**, **Zn-G**) all showed well-defined ^1H NMR spectra, when dissolved in $\text{THF-}d_8$. In contrast, the ^1H NMR spectra of compounds **Zn-D** and **Zn-E** (where $\text{R}_1 = \text{R}_2 = \text{H}$), in $\text{THF-}d_8$ at 298 K, are broad and undefined, thus indicative of higher degrees of aggregation. The use of a stronger donor solvent, pyridine- d_5 , resulted in well-defined ^1H NMR spectra being obtained, consistent with the pyridine coordinating to the zinc centre and favouring the formation of discrete mononuclear complexes. Indeed, there is already a



good literature precedent for the formation of high order clusters/aggregates for unsubstituted (8-quinolinolato)zinc(*tert*-butyl) complexes.¹³ There is also a track record for pyridine coordinating to zinc complexes and disrupting aggregate structures.¹⁴ To further confirm the structures of **Zn-D**, a single crystal X-ray diffraction experiment (*vide infra*) showed the complex exhibited a trimeric structure in the solid state.

X-ray crystallography

Single crystals, suitable for X-ray diffraction experiments, were isolated for compounds **Zn-A**, **Zn-D** and **Al-E** from THF-hexane and toluene solutions, respectively. The crystallizations occurred at $-18\text{ }^{\circ}\text{C}$ for **Zn-D** and **Al-E** and at $25\text{ }^{\circ}\text{C}$ for **Zn-A**. Illustrations of the structures are shown in Fig. 5–8 and Table 1 presents selected bond lengths and angles (for full data see the ESI†).

The structure of the aluminium complex **Al-E** shows a distorted trigonal bipyramidal coordination geometry ($\tau = 0.62$) for the aluminium centre, with N1 and N21 occupying the axial sites (Fig. 5). Both of the C_2NOZn chelate rings have envelope conformations; for the N1/O9 chelate ring the metal lies *ca.* 0.12 Å out of the C_2NO plane (the atoms of which are coplanar to within *ca.* 0.01 Å), whilst for the N21/O29 case the aluminium lies *ca.* 0.18 Å out of the plane of the other four atoms (which are coplanar to better than 0.01 Å).

The structures of the two zinc complexes confirm the formation of aggregates in the solid state, presumably driven in part by the high stability of four coordinate, tetrahedral zinc

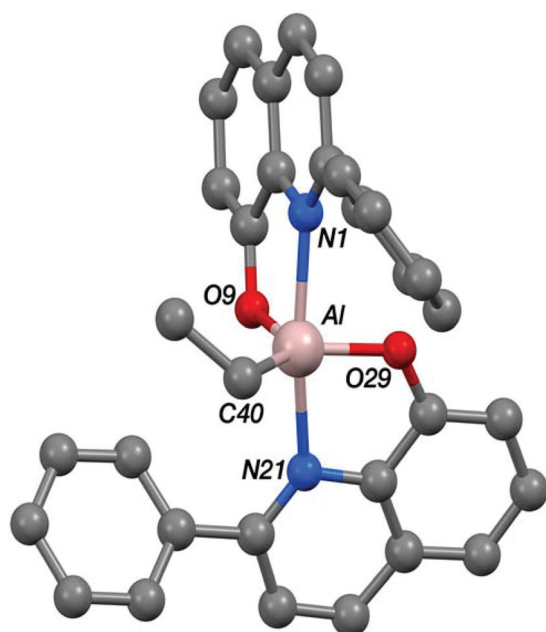


Fig. 5 The crystal structure of **Al-E**. Selected bond lengths (Å) and angles ($^{\circ}$): Al–N1 2.1892(10), Al–O9 1.7989(9), Al–N21 2.1527(10), Al–O29 1.8007(10), Al–C40 1.9746(13), N1–Al–O9 82.28(4), N1–Al–N21 165.14(4), N1–Al–O29 89.27(4), N1–Al–C40 94.77(5), O9–Al–N21 88.62(4), O9–Al–O29 109.02(5), O9–Al–C40 122.89(5), N21–Al–O29 82.59(4), N21–Al–C40 100.04(5), O29–Al–C40 128.02(5).

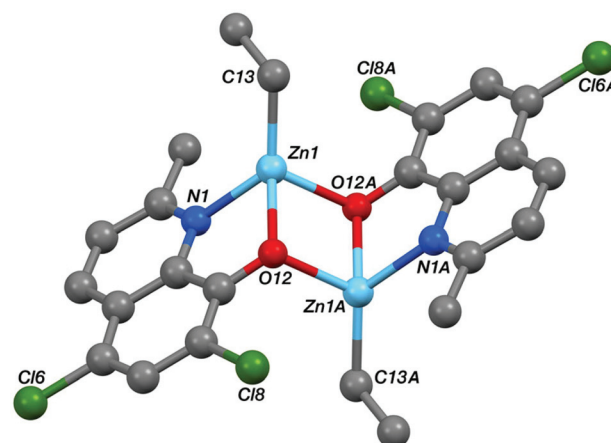


Fig. 6 The crystal structure of the C_i -symmetric complex **Zn-A**. Selected bond lengths (Å) and angles ($^{\circ}$): Zn1–N1 2.0866(17), Zn1–O12 2.0776(14), Zn1–C13 1.984(2), Zn1–O12A 2.0761(15), Zn1...Zn1A 3.09986, N1–Zn1–O12 80.54(6), N1–Zn1–C13 128.80(8), N1–Zn1–O12A 105.43(6), O12–Zn1–C13 129.36(8), O12–Zn1–O12A 83.46(6), C13–Zn1–O12A 117.05(8).

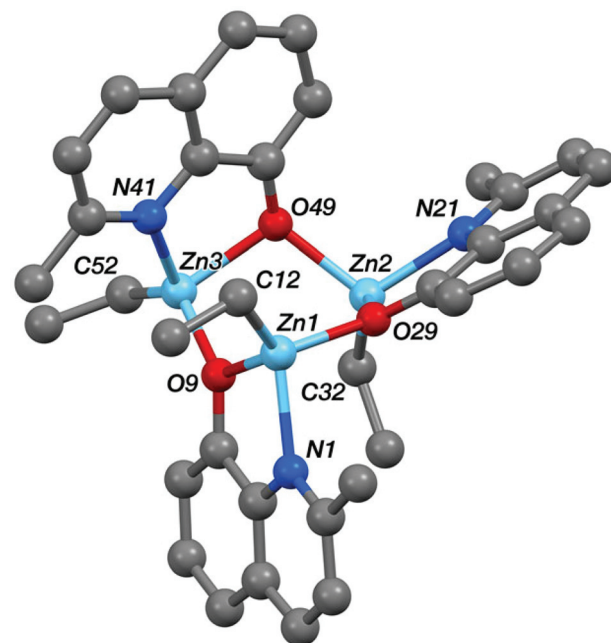


Fig. 7 The crystal structure of **Zn-D**, see Table 1 for selected bond lengths and angles.

centres. The crystal structure of **Zn-A** shows the complex to be a C_i -symmetric dimer with bridging phenoxide oxygen atoms (Fig. 6). The geometry at the zinc centre is noticeably distorted with the angles involving the ethyl ligand all being significantly increased from ideal, ranging between 117.05(8) and 129.36(8) $^{\circ}$. The five-membered C_2NOZn chelate ring has an envelope conformation, the zinc atom lying *ca.* 0.41 Å out of the plane of the other four atoms (which are coplanar to within *ca.* 0.01 Å). In contrast, the crystal structure of **Zn-D** shows a trimeric, cyclic structure based on three EtZn-D units



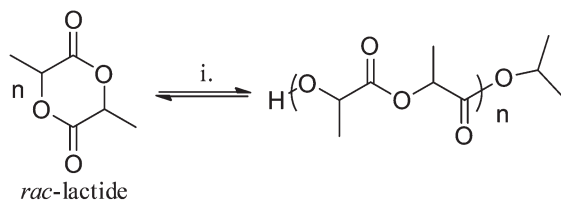


Fig. 8 Illustrates the ring-opening polymerization of lactide to polylactide. Reagents and Conditions: Polymerization conditions: **Al**-(**A–G**): Toluene, 348 K, 1 : 1 : 100 [I] : [iPrOH] : [LA], 1 M [LA]. **Ti**-(**B/D/G**): Toluene, 348 K, 1 : 100 [I] : [LA], 1 M [LA]. **Zn**-(**A–G**): THF/CH₂Cl₂, 298 K, 1 : 1 : 100 [I] : [iPrOH] : [LA], 1 M [LA].

(Fig. 7, Table 1). The Zn₃O₃ ring has a “two-up one-down” arrangement for the quinolinolate ligands; this ring has a twist-boat conformation with Zn3 and O49 lying *ca.* 1.42 and 1.85 Å, respectively, out of the [Zn1, Zn2, O9, O29] plane (which is coplanar to *ca.* 0.11 Å). All three zinc centres have distorted tetrahedral coordination geometries with angles in the ranges 81.20(7)–125.24(10)°, 80.85(7)–128.93(9)° and 80.57(7)–130.87(11)° at Zn1, Zn2 and Zn3 respectively; in each case the smallest angle is the bite of the N,O chelate ligand. Two of the three five-membered C₂NOZn chelate rings are approximately flat (the Zn1 and Zn2 based rings are coplanar to within *ca.* 0.02 and 0.03 Å respectively), whilst the third has an envelope conformation with Zn3 lying *ca.* 0.11 Å out of the plane of the other four atoms which are coplanar to within *ca.* 0.01 Å.

It is notable that ligand **G** contains a redox-active ferrocene substituent and a number of catalysts containing such substituents have been shown to be capable of control/moderation of the polymerization properties by control of ferrocene redox chemistry.^{9g,h,15} Thus, it was relevant to investigate the redox chemistry of compounds **Al-G**, **Ti-G** and **Zn-G**. Cyclic voltammetry showed all three compounds to have reversible redox behaviour, however chemical oxidation proved problematic. Ethyl compounds **Al-G** and **Zn-G** showed evidence of alkyl abstraction using a range of different chemical oxidants including Ag⁺OTf[−], Ag⁺BF₄[−], NO⁺BF₄[−], Fc⁺PF₆[−] and Fc⁺BARF[−], as signalled by the absence of the characteristic ethyl group signals in the ¹H NMR spectra. Attempts to chemically oxidise compound **Ti-G**, a titanium bis(iso-propoxide) species, also failed to result in a paramagnetic Fe(III) species and showed poor stability of any chemically oxidised product formed. As such,

compounds **Al-G**, **Ti-G** and **Zn-G** cannot be redox controlled, rather they are included in this study as initiators containing aromatic/sterically hindered substituents at position R₁.

Ring-opening polymerization of *rac*-lactide

All the new compounds (**Al**, **Zn** and **Ti**) were tested as initiators for the ROP of *rac*-LA and for ease of comparison, the data for **Al**-(**A–D**) is also included (Fig. 8, Table 2).

The polymerizations were conducted under a standard set of conditions; in toluene at 348 K for the aluminium and titanium complexes (note: an equivalent of iso-propyl alcohol was added to polymerizations using aluminium ethyl initiators) or in THF-methylene dichloride, at 298 K, with one equivalent of iso-propyl alcohol for the zinc initiators. All experiments were conducted at a standard concentration of *rac*-lactide (1 M) and using 10 mM concentration of initiator (*i.e.* 1 : 100 loading of initiator : lactide). In the case of the ethyl based initiators, *i.e.* all the **Al** and **Zn** complexes, an equivalent of iso-propyl alcohol was added. This alcohol reacts with the metal ethyl bond, *in situ*, forming an active metal iso-propoxide initiator. The polymerizations are all air and moisture sensitive and so were carried out in a nitrogen filled glovebox or on an argon Schlenk line. The polymerizations were monitored by taking aliquots at regular time intervals. The crude samples (aliquots) were then analysed using ¹H NMR spectroscopy to determine the percentage monomer conversion. Size exclusion chromatography was used to determine the number-averaged molecular weight (*M_n*) and dispersity (PDI) for all samples. The tacticity of the resulting PLA was assessed by integration of the methyne region of the homonuclear decoupled NMR spectrum. The normalized tetrad integrals were compared with the expected probabilities determined by Bernoullian statistics.¹⁶

All the complexes were active initiators in the polymerization of *rac*-LA, the polymerization results are summarised in Tables 2 and 3.

The **Al** and **Ti** initiators showed similar performances, exhibiting slow rates compared to the very best catalysts for lactide polymerization but at values as expected for these metal centres. The polymerization kinetics were monitored for **Al** and **Ti** initiators, showing first order dependencies on lactide concentration in all cases; the pseudo first order rate constants, *k_{obs}*, were obtained as the gradient of the linear fits to plots of ln([LA]₀/[LA]_{*t*}) versus time (Fig. 9, 10 and ref. 10*b* for the data for **Al**-(**A–D**)). Of the **Al** compounds, **Al-E** (R₃ = Ph)

Table 1 Selected bond lengths (Å) and angles (°) for **Zn-D**

Zn1–N1	2.083(2)	Zn2–N21	2.083(2)	Zn3–N41	2.097(2)
Zn1–O9	2.0514(17)	Zn2–O29	2.0487(16)	Zn3–O49	2.0537(16)
Zn1–C12	1.975(3)	Zn2–C32	1.977(3)	Zn3–C52	1.979(3)
Zn1–O29	2.0215(16)	Zn2–O49	2.0427(17)	Zn3–O9	2.0116(17)
N1–Zn1–O9	81.20(7)	N21–Zn2–O29	80.85(7)	N41–Zn3–O49	80.57(7)
N1–Zn1–C12	123.03(10)	N21–Zn2–C32	125.24(10)	N41–Zn3–C52	123.88(11)
N1–Zn1–O29	101.28(7)	N21–Zn2–O49	108.13(7)	N41–Zn3–O9	95.85(7)
O9–Zn1–C12	125.24(10)	O29–Zn2–C32	128.93(9)	O49–Zn3–C52	115.50(10)
O9–Zn1–O29	94.00(7)	O29–Zn2–O49	95.89(7)	O49–Zn3–O9	96.95(7)
C12–Zn1–O29	122.22(10)	C32–Zn2–O49	111.70(9)	C52–Zn3–O9	130.87(11)



Table 2 Polymerization data obtained using initiators Al-(A–G) and Ti-B, D, G

Initiator (I)	Time (h)	Convsn. ^d (%)	$k_{\text{obs}} \times 10^{-6} \text{ s}^{-1} \text{ }^e$	$M_n \text{ }^f (\text{g mol}^{-1})$	$M_{n, \text{calc}}$	$\text{PDI} \text{ }^f$	$P_i \text{ }^g$
Al-A ^a	137	91	5.0	9900	13 100	1.11	0.72
Al-B ^a	169	80	2.5	7000	11 500	1.04	0.75
Al-C ^a	168	90	4.2	12 400	12 900	1.07	0.75
Al-D ^a	169	94	4.3	9300	13 500	1.19	0.62
Al-E ^b	28	91	24	9700	13 100	1.11	0.56
Al-F ^b	165	93	4.3	10 500	13 400	1.13	0.75
Al-G ^b	288	88	2.2	12 700	12 700	1.05	0.66
Ti-B ^c	186	91	3.7	5400	6550	1.14	0.65
Ti-D ^c	258	82	2.0	5600	5900	1.06	0.61
Ti-G ^c	308	85	1.7	6600	6100	1.08	0.63

^a The results are reproduced from ref. 10b to enable comparisons between the initiators. ^b Polymerization conditions: Toluene, 348 K, 1 : 1 : 100 [I] : [iPrOH] : [LA], 1 M [LA]. ^c Toluene, 348 K, 1 : 100 [I] : [LA], 1 M [LA]. ^d Determined by integration of the methine region of the ¹H NMR spectrum (LA 4.98–5.04 ppm; PLA 5.08–5.22 ppm). ^e Determined from the gradients of the plots of $\ln\{[LA]_0/[LA]_t\}$ versus time. ^f Determined by GPC-SEC in THF, using a correction factor of 0.58. ^g Determined by analysis of all the tetrad signals in the methine region of the homonuclear decoupled ¹H NMR spectrum.

Table 3 Polymerization data obtained using initiators Zn-A–E and G

I ^a	Solv.	Time (min)	Conv. ^b (%)	$k_{\text{obs}} \times 10^{-4} \text{ s}^{-1} \text{ }^c$	$M_{n, \text{theo.}}$	$M_{n, \text{NMR}} \text{ }^d (\text{g mol}^{-1})$	$M_{n, \text{LS}} \text{ }^e (\text{g mol}^{-1})$	$M_{n, \text{SEC}} \text{ }^f (\text{g mol}^{-1})$	$\text{PDI} \text{ }^{e,f}$	$P_s \text{ }^g$
Zn-A	THF	445	91	1.4	13 100	12 600	11 000	7400	1.10	0.66
Zn-A	DCM	260	90	1.7	13 000	8500	8900	5600	1.03	0.60
Zn-B	THF	240	90	2.1	13 000	8750	8700	—	1.06	0.66
Zn-B	DCM	200	92	2.4	13 250	8750	9000	—	1.03	0.60
Zn-C	THF	370	93	1.6	13 400	8000	9400	6200	1.03	0.66
Zn-C	DCM	290	95	1.8	13 700	9900	9100	6400	1.08	0.60
Zn-D	THF	560	85	0.8	12 300	—	8000	7000	1.07	0.67
Zn-E	THF	460	89	1.0	12 800	6600	7500	5700	1.10	0.70
Zn-G	THF	480	93	0.9	13 400	6700	10 000	—	1.09	0.65

^a Polymerization conditions: 298 K, 1 : 1 : 100 [I] : [iPrOH] : [LA], 1 M [LA]. ^b Determined by integration of the methine region of the ¹H NMR spectrum (LA 4.98–5.04 ppm; PLA 5.08–5.22 ppm). ^c Determined from the gradients of the plots of $\ln\{[LA]_0/[LA]_t\}$ versus time. ^d Determined by integration of the hydroxyl chain-end versus the polymer methine protons. ^e Determined by GPC in THF, using multiangle laser light scattering (GPC-MALLS). ^f Determined by GPC in THF versus polystyrene standard and a correction factor on 0.58. ^g Determined by analysis of all the tetrad signals in the methine region of the homonuclear decoupled ¹H NMR spectrum.

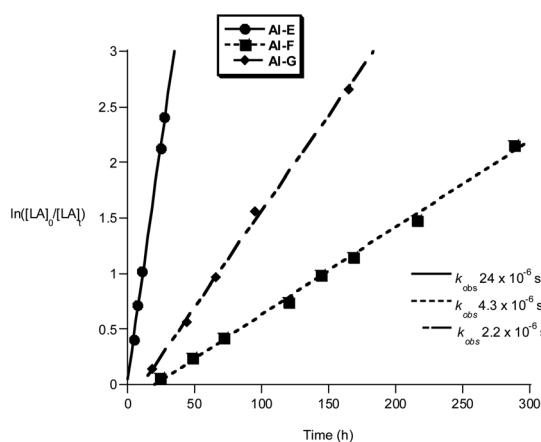


Fig. 9 Plot of $\ln\{[LA]_0/[LA]_t\}$ vs. time of initiator Al-E, F and G. Conditions: $[LA]_0 = 1 \text{ M}$, 1 : 1 : 100 [I] : [iPrOH] : [LA], toluene, 348 K.

stands out as having a significantly faster rate ($k_{\text{obs}} = 24 \times 10^{-6} \text{ s}^{-1}$), it is also notable that a similarly higher rate was observed when $R_3 = t\text{Bu}$ as previously reported by us ($k_{\text{obs}} = 58 \times 10^{-6} \text{ s}^{-1}$).^{10b} It seems that the substitution at R_3 position exerts

more of an electronic influence on the aluminium centre, than substitution at sites R_1 or R_2 . The other initiators Al-F and Al-G have comparable rates to the previously reported Al-(A–D).^{10b} It is notable that compound Al-F has a short lag period at the start of the polymerization, likely owing to a relatively slow formation of the active aluminium alkoxide initiating species.

The titanium complexes, Ti-B, D and G were all slow initiators with comparable observed rate constants to the Al initiators ($k_{\text{obs}} = 1.7\text{--}3.7 \times 10^{-6} \text{ s}^{-1}$). It is interesting to note that the rate of polymerisation of Ti-B was faster than Ti-D, the opposite trend to that observed for the aluminium complexes bearing the same ligands. The slower rate of polymerization of compounds Ti-B and Ti-G, versus Ti-D (where $R_1 = R_2 = \text{H}$), could have a steric origin *note*: limited electronic trends with variation of R_1 and R_2 could be identified in the series of related aluminium complexes. The data for the kinetics of Ti-G show a slight deviation from linearity ($R^2 = 0.9577$) which is proposed to be due to the relatively long polymerization period and/or slower initiation.

Compounds Al-E, F and G exhibited a high degree of polymerization control, with all initiators showing a linear evolution of molecular weight with percentage conversion, M_n



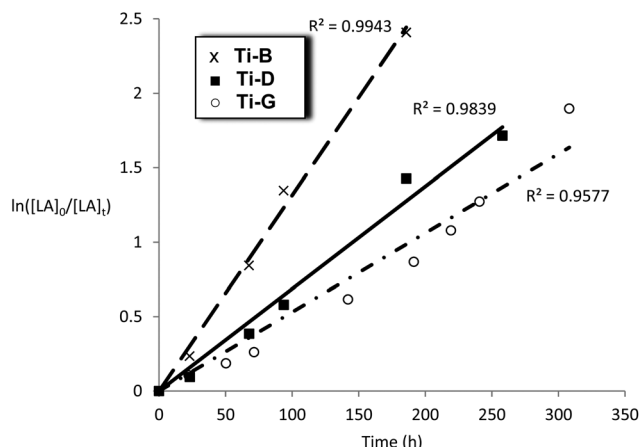


Fig. 10 Plot of $\ln([LA]_0/[LA]_t)$ vs. time for initiators Ti-B, D and G. Conditions: $[LA]_0 = 1\text{ M}$, 1 : 100 [I] : [LA], toluene, 348 K.

values being close to those predicted on the basis of the initiator concentration and dispersities are narrow throughout the course of the polymerizations (<1.11 in all cases). This level of polymerization control is comparable to the previously reported bis(8-quinolinolato)aluminium ethyl compounds and the bis(8-quinolinolato)gallium *tert*-butoxide compounds.^{10a,b} The polymer end-groups were analysed using MALDI-ToF mass spectrometry, which showed that the major series were chain end-capped with iso-propyl ester groups (Fig. S18†). Compounds Ti-B, D and G also show a linear evolution of number averaged molecular weight (M_n) and narrow dispersities. The M_n values were consistent with two polymer chains growing from the two alkoxide initiating groups on the titanium catalysts (Table 2). This is rather different to the aluminium catalysts where a single polymer chain grows (for the single alkyl site). Thus, although equivalent rates are exhibited per equivalent of metal, the rate of the aluminium per active site is likely faster (approximately twice as fast).

The Al and Ti initiators all exert an isotactic bias during the polymerization of *rac*-LA. It is observed that the initiators with

the most sterically hindered substituents at the R_1 position result in higher degrees of iso-selectivity, *i.e.* Al-A, Al-B and Al-F. For the new initiators the best iso-selectivity is observed for Al-F ($P_i = 0.75$), with a phenyl substituent at R_1 . Attempts to prepare related ligands with more sterically hindered substituents at R_1 were unsuccessful due to problems with ligand synthesis/purification. The analysis of the isotactic PLA produced by Al-F indicates that an enantiomorphic site control mechanism is dominant, with the relative integrals of stereoerror signals being: [sis]:[sii]:[iis]:[isi] = 1 : 1 : 1 : 2 (Fig. S19†). Compared to the Al analogues, the Ti complexes show lower iso-selectivities, with the maximum $P_i = 0.65$ for Ti-B (Fig. S20†). It should be noted that any degree of iso-selectivity for titanium initiators is rather unusual and this value may represent an interesting opportunity to prepare more selective titanium initiators in the future.¹⁷ In contrast, there have been several previous examples of hetero-selective titanium initiators and in such cases, the selectivity has been improved using heavier Group (IV) complexes, *i.e.* of Zr(IV) or Hf(IV).^{9d-f,i,j,18}

Polymerizations were also conducted using the Zn initiators, either in methylene dichloride or THF solutions at 298 K (Table 3).

The polymerization kinetics were monitored for each initiator and show a first order dependence on lactide concentration in every case. The pseudo first-order rate constants, k_{obs} , were determined when the polymerization was conducted in either THF (Fig. 11) or methylene dichloride (Fig. 12). In contrast to the Al initiators which require thermal activation, the Zn initiators are all active at 298 K. It may be that for the Al initiators, the higher temperatures are required to accelerate the formation of the active aluminium alkoxide species, whereas for the zinc initiators the reaction between alcohol and zinc-ethyl occurs without heating. Such a proposal is supported by the reduced bond dissociation energy of zinc-carbon bonds, Zn-C₂H₅ 201 kJ mol⁻¹, compared to aluminium-carbon bonds, Al-C 255 kJ mol⁻¹.¹⁹

The polymerizations in THF exhibited a significant induction period (~1–2 hours), after which the polymerizations pro-

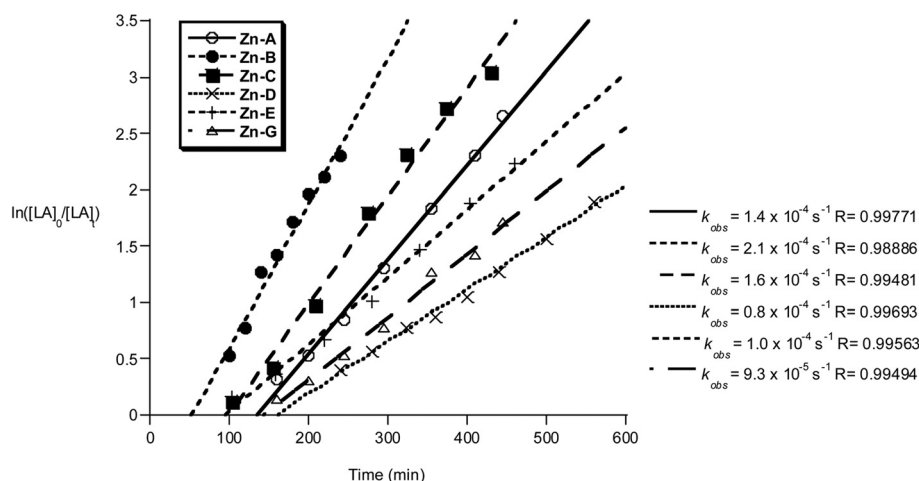


Fig. 11 Plot of $\ln([LA]_0/[LA]_t)$ vs. time of initiator Zn-A–E and G. Conditions: $[LA]_0 = 1\text{ M}$, 1 : 1 : 100 [I] : [iPrOH] : [LA], THF, 298 K.



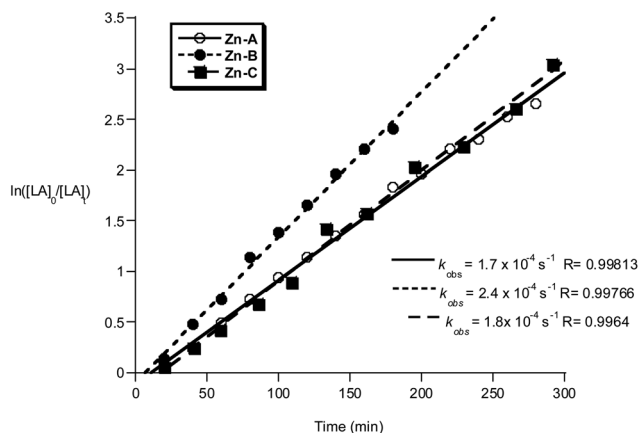


Fig. 12 Plot of $\ln([LA]_0/[LA]_t)$ vs. time of initiators **Zn-A**, **B** and **C**. Conditions: $[LA]_0 = 1\text{ M}$, $1 : 1 : 100$ [I] : [iPrOH] : [LA], CH_2Cl_2 , 298 K .

gressed with good control and showed pseudo first-order kinetics. Interestingly, when methylene dichloride was employed as a solvent, the induction period was not observed. It is proposed that during the induction period, the active alkoxide initiator is forming and that THF coordination may slow the rate of Zn-C alcoholysis. During the propagation phases the rates of polymerization are not significantly influenced by the reaction solvent, with comparable values for k_{obs} being obtained (**Zn-A**: $k_{\text{obs}} = 1.4 \times 10^{-4}\text{ s}^{-1}$ in THF and $k_{\text{obs}} = 1.7 \times 10^{-4}\text{ s}^{-1}$ in methylene chloride). The polymerization activity of compounds **Zn-D**, **Zn-E** and **Zn-G** in methylene dichloride were not monitored, due to the reduced solubility of the initiator in that solvent.

The zinc compounds were moderately fast initiators, reacting in the order **Zn-B** > **Zn-C** > **Zn-A** > **Zn-E** > **Zn-G** > **Zn-D**. Compounds **Zn-A**, **Zn-B** and **Zn-C** (where $R_1 = R_2 = \text{Cl}$, $R_1 = \text{I}$, $R_2 = \text{Cl}$ and $R_1 = R_2 = \text{Br}$, respectively) were the fastest, with a clear trend in rate with respect to the halide substituent $\text{I} > \text{Br} > \text{Cl}$ and with the Lewis acidity of the active site. In contrast to the results using Al initiators, compound **Zn-E** ($R_3 = \text{Ph}$), is slightly slower than the other Zn initiators. This suggests that different factors govern the activity of the two types of metal initiator. A comparison of the activity of these Zn initiators with other known literature systems reveals them to be of good rate (for Zn compounds). They show equivalent activity to Schiff base zinc complexes and zinc guanidinate complexes.²⁰ They are faster than zinc ketoiminate compounds ($1 : 100$ I : [LA], 298 K , chloroform, 24 h , 100%), which also contain a quinolinolate ligand system.²¹ However, compared to the very best zinc catalysts, based on phenolate diamines/diimines, the activities of these Zn compounds are significantly lower.²²

All the Zn initiators show a linear evolution of M_n with percentage conversion, and the dispersities are narrow throughout the polymerizations (<1.10 in all cases). The polymer molecular weights were compared using different size exclusion chromatographic methods, either as an absolute value using light scattering, or vs. polystyrene standards (with correction factors applied) or by $^1\text{H NMR}$ analysis (by comparison of

the signals for the main chain vs. the iso-propoxide end group). In all cases the values are slightly lower than expected. There is no significant initiation from the quinolinolate moieties on the ligand, as determined by $^1\text{H NMR}$ and MALDI-ToF analysis of the PLA end-groups. The end group analysis using MALDI-ToF mass spectrometry, showed just one major series in which the chains were end-capped with iso-propyl ester groups and the peaks are separated by 144 amu , consistent with only limited inter-molecular transesterification occurring (Fig. S21†).

Compounds **Zn-A-E** and **G** polymerize *rac*-LA with a slight heterotactic bias, maximum $P_s = 0.70$ (Fig. S22†). The degree of stereocontrol does not change as the substituents at the R_1 position are altered, this is in contrast to the ability to use this site to ‘tune’ the iso-selectivity of the Al initiators. Slightly increased hetero-selectivity was observed when the polymerizations are conducted in THF vs. methylene dichloride, $P_s = 0.66$ vs. 0.60 for both compounds **Zn-A**, **B** and **C**. This improvement in stereocontrol when THF is employed as a solvent has been observed for many other initiating systems.²³ It has been postulated that the labile coordination of THF to the Lewis acidic metal centres facilitates the hetero-selectivity.^{23a,24}

Conclusions

This study investigated the preparation of a series of new compounds of various 8-hydroxyquinoline ligands with earth-abundant metals, including Al(III), Ti(IV) and Zn(II). The proligands contained different substituents at positions *ortho* (R_1) and *para* (R_2) to the phenolate and *ortho* (R_3) to the N moieties. The coordination chemistry resulted in the formation of bis(8-quinolinolato)aluminium ethyl, bis(8-quinolinolato) bis(iso-propoxide) titanium(IV) and (8-quinolinolato)-zinc(II) ethyl complexes which were characterized using spectroscopy, elemental analysis and, in some cases, using single crystal X-ray diffraction experiments. In the case of Al complexes, the coordination geometries were distorted trigonal bipyramidal, with the N-atoms occupying the axial sites. In the case of the zinc complexes, dimeric or higher order aggregates (trimer) were formed depending on the ligand substitution.

All the new complexes were active initiators, in the cases of metal alkyl complexes in combination with exogenous alcohol, for lactide polymerization. The Al and Ti initiators showed similar rates which were typical for those particular metal centres. The Zn initiators, which operated under milder conditions, showed good rates which were significantly (qualitatively) faster than the Al/Ti analogues. In terms of the ligand substitution influences over the polymerization rates, the Al complexes showed significantly faster rates if the position *ortho* to the N atom, on the ligand, was substituted with a sterically hindered group. In contrast, for the Zn initiators no such effect was observable. The complexes all exerted high degrees of polymerization control, leading to PLA of predictable M_n with narrow dispersity (<1.11 in all cases). Furthermore, the Al and Ti initiators exhibited moderate iso-selectivities ($P_i = 0.75$)



whilst the Zn initiators showed a moderate hetero-selectivities ($P_s = 0.70$).

This series of complexes demonstrates the potential and versatility of the 8-hydroxyquinoline ligand type; ligands which can be easily prepared and offer multiple sites for substitution. The experiments demonstrate the potential for good control, moderate rates and, in some cases, stereocontrol using this ligand class and earth-abundant metals. The influence of the metal coordination spheres over rate and stereochemistry differs from Al/Ti to Zn and this warrants further investigation in the future to help to understand the critical factors to prepare improved catalysts.

Experimental section

All reactions were conducted under an inert nitrogen atmosphere, using a nitrogen filled glovebox or standard Schlenk techniques. The pro-ligands **A–D** were prepared as previously described,^{10b} whilst the experimental protocols for pro-ligands **E–G** are reported in the ESI.† All solvents and reagents were obtained from commercial sources. Triethyl aluminium and diethyl zinc were obtained from Strem and titanium(IV) *tetrakis*-(iso-propoxide) was obtained from Sigma-Aldrich. Toluene and THF was distilled from sodium, de-gassed and stored under nitrogen. Methylene dichloride was distilled from CaH₂. Isopropyl alcohol was heated to reflux over CaH₂, distilled onto fresh CaH₂ and further refluxed, then distilled, degassed and stored under nitrogen. Benzene-*d*₆ was distilled from sodium, THF-*d*₈, toluene-*d*₈ and CDCl₃ were dried over CaH₂, and all were then degassed and stored under nitrogen. *rac*-Lactide was obtained from Purac Plc. and was crystallised from dry toluene and sublimed at 323 K three times under vacuum.

Nuclear magnetic resonance (NMR) spectra were recorded on a Bruker Av400 spectrometer operating at 400 MHz for ¹H and 100 MHz for ¹³C{¹H} spectra. Solvent peaks were used as internal references for ¹H and ¹³C chemical shifts (ppm). Higher resolution ¹H NMR and ¹H{¹H} NMR (homo-decoupled spectroscopy) experiments were performed on a Bruker Av500 spectrometer and also a DRX 400 spectrometer by Mr Peter Haycock. Spectra were processed and analyzed using Mestrenova software. MALDI-ToF mass spectra were performed on a Waters/Micromass MALDI micro MX, using potassium or sodium salts for ionization. Elemental analyses were determined by Mr Stephen Boyer at London Metropolitan University, Science Centre, 29 Hornsey Road, London N7 7DD. GPC-MALLS measurements were conducted on a Polymer Laboratories PL GPC-50 instrument at 35 °C, using two Polymer Laboratories Mixed D columns in series and THF as the eluent, at a flow rate of 1 mL min^{−1}. The light scattering detector was a Dawn 8, Wyatt Technology, and data were analysed using Astra V version 5.3.4.18.

Aluminium complexes

Triethyl aluminium (53 mg, 0.46 mmol) in toluene (5 mL) was added, drop-wise with stirring, to a solution of the desired

8-hydroxyquinoline (0.93 mmol) in toluene (10 mL). The reaction was stirred for 12 h, after which time the solvent was removed *in vacuo*. The resulting solid was washed with hexane, filtered, and dried *in vacuo* to yield a yellow powder.

Compound Al-E. ¹H NMR (500 MHz, THF-*d*₈) δ (ppm): 8.49 (d, 2H, CH, ³*J*_{HH} = 8.5 Hz), 8.26 (dt, 4H, CH, ³*J*_{HH} = 7.0 Hz, ⁴*J*_{HH} = 1.7 Hz), 7.75 (d, 2H, CH, ³*J*_{HH} = 8.5 Hz), 7.48 (t, 2H, CH, ³*J*_{HH} = 8.2 Hz), 7.40 (m, 6H, CH^(4H), CH^(2H)), 7.24 (dd, 2H, CH, ³*J*_{HH} = 8.2 Hz, ⁴*J*_{HH} = 1.2 Hz), 7.04 (dd, 2H, CH, ³*J*_{HH} = 7.5 Hz, ⁴*J*_{HH} = 1.2 Hz), −0.21 (t, 3H, CH₂CH₃, ³*J*_{HH} = 8.0 Hz), −1.08 (dq, 2H, CH₂CH₃, ³*J*_{HH} = 8.0 Hz, ⁴*J*_{HH} = 2.0 Hz); ¹³C {¹H} NMR (100 MHz, THF-*d*₈) δ (ppm): 159.4 (C^{IV}), 158.6 (C^{IV}), 141.5 (C^{IV}), 140.5 (C^{IV}), 140.2 (CH), 131.2 (CH), 131.2 (CH), 130.8 (CH), 130.1 (CH), 129.4 (C^{IV}), 129.2 (CH), 125.0 (CH), 114.5 (CH), 113.9 (CH), 9.3 (CH₃), 1.8 (CH₂); Anal. Calc. (AlC₃₂H₂₅N₂O₂): C, 77.40; H, 5.07; N, 5.64 Found: C, 77.48; H, 5.20; N, 5.68.

Compound Al-F. ¹H NMR (400 MHz, benzene-*d*₆) δ (ppm): 7.97 (d, 2H, CH, ³*J*_{HH} = 8.6 Hz), 7.74 (d, 2H, CH, ³*J*_{HH} = 8.6 Hz), 7.63 (s, 2H, CH), 7.18–7.29 (m, 8H, CH), 6.56 (d, 2H, CH, ³*J*_{HH} = 8.6 Hz), 2.80 (s, 6H, CH₃), 1.05 (t, 3H, CH₂CH₃, ³*J*_{HH} = 8.13 Hz), 0.50–0.62, 0.30–0.43 (m, 2H, CH₂CH₃); ¹³C {¹H} NMR (100 MHz, benzene-*d*₆) δ (ppm): 157.6 (C^{IV}), 153.95 (C^{IV}), 141.1 (C^{IV}), 138.5 (C^{IV}), 135.7 (CH), 130.0 (CH), 129.9 (CH), 127.8 (CH), 127.1 (CH), 125.4 (C^{IV}), 124.4 (C^{IV}), 124.1 (CH), 116.9 (C^{IV}), 23.2 (CH₃), 9.9 (CH₂CH₃), 1.4 (CH₂CH₃); Anal. Calc. (C₃₄H₂₇AlCl₂N₂O₂): C, 68.81; H, 4.59; N, 4.72 Found: C, 68.60; H, 4.71; N, 4.82.

Compound Al-G. ¹H NMR (400 MHz, THF-*d*₈) δ (ppm): 8.59 (d, 2H, CH, ³*J*_{HH} = 8.8 Hz), 7.79 (d, 2H, CH, ³*J*_{HH} = 8.8 Hz), 7.57 (s, 2H, CH), 4.49 (t, 4H, (Cp(CH)C≡C), ³*J*_{HH} = 2.0 Hz), 4.27 (t, 4H, (Cp(CH)C≡C), ³*J*_{HH} = 2.0 Hz), 4.19 (s, 10H, Cp(CH)), 3.34 (s, 6H, CH₃), 0.67 (t, 3H, CH₃, ³*J*_{HH} = 8.0 Hz), 0.11 (dq, 2H, CH₂, ³*J*_{HH} = 8.0 Hz, ⁴*J*_{HH} = 14.6 Hz); ¹³C{¹H} NMR (100 MHz, toluene-*d*₈) δ (ppm): 158.8 (C^{IV}), 158.2 (C^{IV}), 140.5 (C^{IV}), 135.8 (CH), 131.0 (CH), 124.7 (C^{IV}), 124.6 (CH), 116.2 (C^{IV}), 109.1 (C^{IV}), 93.7 (C≡C), 83.7 (C≡C), 71.7 (Cp(CH)C≡C), 70.3 (Cp(CH)), 69.8 (Cp(CH)C≡C), 66.8 (Cp(C^{IV})C≡C), 23.3 (CH₃), 9.9 (CH₂CH₃), 1.4 (CH₂CH₃); Anal. Calc. (AlC₄₆H₃₅Cl₂Fe₂N₂O₂): C, 64.44; H, 4.11; N, 3.27 Found: C, 64.35; H, 4.05; N, 3.27.

Titanium complexes

Titanium(IV) *tetrakis*(iso-propoxide) (0.23 mL, 0.80 mmol) in toluene (15 mL) was added, drop-wise under nitrogen, to a solution of the 8-hydroxyquinoline (1.6 mmol) in toluene (15 mL), with stirring. The clear yellow solution was left to stir for 12 h at 298 K. The solvent was removed *in vacuo* and the product washed with hexane (10 mL) and isolated as a yellow solid.

Compound Ti-B. ¹H NMR (400 MHz, chloroform-*d*) δ (ppm): 8.24 (d, 2H, CH, ³*J*_{HH} = 8.7 Hz), 7.86 (s, 2H, CH), 7.17 (d, 2H, CH, ³*J*_{HH} = 8.7 Hz), 5.02 (sept, 2H, CH), 2.82 (s, 6H, CH₃), 1.28 (dd, 12H, CH₃); ¹³C{¹H} NMR (100 MHz, chloroform-*d*) δ (ppm): 160.8 (C^{IV}), 160.3 (C^{IV}), 140.6 (C^{IV}), 135.3 (CH), 134.9 (CH), 125.2 (C^{IV}), 125.01 (CH), 117.6 (C^{IV}), 80.6 (CH), 79.4 (C^{IV}), 26.6 (CH₃), 24.1 (CH₃); Anal. Calc.



(C₂₆H₂₆Cl₂I₂N₂O₄Ti): C, 38.89%; H, 3.26%; N, 3.49%. Found: C, 38.68%; H, 3.17%; N, 3.42%.

Compound Ti-D. ¹H NMR (400 MHz, benzene-*d*₆) δ (ppm): 7.24 (t, 2H, CH, ³J_{HH} = 8.0 Hz), 7.15 (d, 2H, CH, ³J_{HH} = 8.7 Hz), 7.05 (dd, 2H, CH, ³J_{HH} = 7.6 Hz, ⁴J_{HH} = 1.2 Hz), 6.75 (dd, 2H, CH, ³J_{HH} = 8.0 Hz, ⁴J_{HH} = 0.8 Hz), 6.30 (d, 2H, CH, ³J_{HH} = 8.4 Hz), 5.10 (sept, 2H, CH, ³J_{HH} = 6.0 Hz), 2.94 (s, 6H, CH₃), 1.31 (dd, 12H, CH₃, ³J_{HH} = 6.0 Hz); ¹³C{¹H} NMR (100 MHz, chloroform-*d*) δ (ppm): 161.3 (C^{IV}), 158.7 (C^{IV}), 142.5 (C^{IV}), 137.1 (CH), 127.8 (CH), 127.6 (C^{IV}), 123.9 (CH), 114.6 (CH), 111.7 (CH), 79.0 (CH), 25.4 (CH₃), 23.2 (CH₃); Anal. Calc. (C₂₆H₃₀N₂O₄Ti): C, 64.74%; H, 6.27%; N, 5.81%. Found: C, 64.66%; H, 6.34%; N, 5.69%.

Compound Ti-G. ¹H NMR (400 MHz, benzene-*d*₆) δ (ppm): 7.68 (s, 1H, CH), 7.64 (d, 1H, CH, ³J_{HH} = 8.4 Hz), 6.26 (d, 1H, CH, ³J_{HH} = 8.4 Hz), 5.19 (sept, 2H, CH, ³J_{HH} = 6 Hz), 4.62 (m, 2H, Cp(CH)), 4.25 (s, 5H, Cp(CH)), 4.05 (m, 2H, Cp(CH)), 3.06 (s, 3H, CH₃), 1.49 (d, 6H, CH₃, ³J_{HH} = 6 Hz), 1.41 (d, 6H, CH₃, ³J_{HH} = 6 Hz); ¹³C{¹H} NMR (100 MHz, chloroform-*d*) δ (ppm): 160.2 (C^{IV}), 142.6 (C^{IV}), 134.4 (CH), 129.8 (CH), 124.9 (CH), 124.9 (C^{IV}), 116.9 (C^{IV}), 107.2 (C^{IV}), 93.8 (C^{IV}), 83.2 (C≡C), 80.1 (C≡C), 71.4 (CH), 71.3 (Cp(CH)), 70.1 (Cp(CH)), 68.9 (Cp(CH)), 66.0 (Cp(C)), 25.6 (CH₃), 23.6 (CH₃); Anal. Calc. (C₅₀H₄₄Cl₂I₂-N₂O₄Ti): C, 62.08%; H, 4.58%; N, 2.90%. Found: C, 61.93%; H, 4.57%; N, 2.99%.

Zinc complexes

Diethyl zinc (0.27 g, 2.19 mmol) in toluene (5 mL) was added, dropwise with stirring, to a solution of 8-hydroxyquinoline (2.19 mmol) in toluene (15 mL). The solution was stirred for 12 h, after which time a yellow precipitate had formed. The precipitate was isolated by filtration, washed with hexane and dried *in vacuo* to yield a yellow solid.

Compound Zn-A. ¹H NMR (400 MHz, THF-*d*₈) δ (ppm): 8.51 (d, 1H, ³J_{HH} = 8.6 Hz), 7.56 (d, 1H, ³J_{HH} = 8.6 Hz), 7.55 (s, 1H), 2.84 (s, 3H), 1.31 (t, 3H, ³J_{HH} = 8.2 Hz), 0.43 (q, 2H, ³J_{HH} = 8.2 Hz); ¹³C{¹H} NMR (125.3 MHz, THF-*d*₈) δ (ppm): 160.0 (C^{IV}), 157.6 (C^{IV}), 141.4 (C^{IV}), 137.3 (CH), 130.4 (CH), 125.4 (C^{IV}), 123.9 (CH), 118.2 (C^{IV}), 112.0 (C^{IV}), 24.7 (CH₃), 13.3 (CH₂CH₃), -1.5 (CH₂CH₃); Anal. Calc. (ZnC₁₂H₁₁NOCl₂): C, 44.83%; H, 3.45%; N, 4.36%. Found: C, 44.88%; H, 3.33%; N, 4.28%.

Compound Zn-B. ¹H NMR (400 MHz, THF-*d*₈) δ (ppm): 8.50 (d, 1H, CH, ³J_{HH} = 8.6 Hz), 7.84 (s, 1H, CH), 7.59 (d, 1H, CH, ³J_{HH} = 8.6 Hz), 2.84 (s, 3H, CH₃), 1.31 (t, 3H, CH₃, ³J_{HH} = 8.2 Hz), 0.43 (q, 2H, CH₂, ³J_{HH} = 8.2 Hz); ¹³C{¹H} NMR (125.3 MHz, THF-*d*₈) δ (ppm): -1.3 (CH₂CH₃), 13.3 (CH₂CH₃), 24.8 (CH₃), 81.9 (C^{IV}), 113.2 (C^{IV}), 124.2 (CH), 126.4 (C^{IV}), 137.5 (CH), 137.5 (CH), 138.8 (C^{IV}), 157.7 (C^{IV}), 163.7 (C^{IV}); Anal. Calc. (ZnC₁₂H₁₁ClINO): C, 34.90%; H, 2.68%; N, 3.39%. Found: C, 34.84%; H, 2.64%; N, 3.31%.

Compound Zn-C. ¹H NMR (400 MHz, THF-*d*₈) δ (ppm): 8.46 (d, 1H, CH, ³J_{HH} = 8.4 Hz), 7.85 (s, 1H, CH), 7.57 (d, 1H, CH, ³J_{HH} = 8.4 Hz), 2.84 (s, 3H, CH₃), 1.31 (t, 3H, CH₃, ³J_{HH} = 8.0 Hz), 0.43 (q, 2H, CH₂, ³J_{HH} = 8.0 Hz); ¹³C{¹H} NMR (125.3 MHz, THF-*d*₈) δ (ppm): 161.4 (C^{IV}), 157.2 (C^{IV}), 141.2

(C^{IV}), 139.8 (CH), 135.8 (CH), 127.1 (C^{IV}), 124.3 (CH), 108.2 (C^{IV}), 100.9 (C^{IV}), 24.1 (CH₃), 13.3 (CH₂CH₃), -1.4 (CH₂CH₃); Anal. Calc. (ZnC₁₂H₁₁Br₂NO): C, 35.12%; H, 2.70%; N, 3.41%. Found: C, 35.25%; H, 2.67%; N, 3.39%.

Compound Zn-D. ¹H NMR (400 MHz, pyridine-*d*₅) δ (ppm): 8.12 (d, 1H, CH, ³J_{HH} = 8.4 Hz), 7.58 (t, 1H, CH, ³J_{HH} = 8.0 Hz), 7.44 (dd, 1H, CH, ³J_{HH} = 8.0 Hz, ⁴J_{HH} = 0.8 Hz), 7.15 (d, 1H, CH, ³J_{HH} = 8.4 Hz), 7.03 (dd, 1H, CH, ³J_{HH} = 8.0 Hz, ³J_{HH} = 0.8 Hz), 2.62 (s, 3H, CH₃), 1.66 (t, 3H, CH₂CH₃, ³J_{HH} = 8.0 Hz), 0.86 (q, 2H, CH₂CH₃, ³J_{HH} = 8.0 Hz); ¹³C{¹H} NMR (100 MHz, THF-*d*₈) δ (ppm): 166.1 (C^{IV}), 154.7 (C^{IV}), 141.57 (C^{IV}), 139.9 (CH), 130.7 (CH), 129.4 (C^{IV}), 122.8 (C^{IV}), 114.5 (CH), 114.5 (CH), 110.2 (CH), 24.8 (CH₃), 14.59 (CH₂CH₃), -1.56 (CH₂CH₃); Anal. Calc. (ZnC₁₂H₁₃NO): C, 57.05%; H, 5.19%; N, 5.54%. Found: C, 57.00%; H, 5.24%; N, 5.67%.

Compound Zn-E. ¹H NMR (400 MHz, pyridine-*d*₅) δ (ppm): 8.30 (d, 1H, CH, ³J_{HH} = 8.8 Hz), 7.76 (d, 2H, CH, ³J_{HH} = 6.8 Hz, ⁴J_{HH} = 2.2 Hz), 7.66 (t, 1H, CH, ³J_{HH} = 8.0 Hz), 7.58 (d, 1H, ³J_{HH} = 8.4 Hz), 7.52 (m, 4H, CH, CH, CH), 7.10 (dd, 1H, CH, ³J_{HH} = 8.0 Hz, ⁴J_{HH} = 1.0 Hz), 1.34 (t, 3H, CH₂CH₃, ³J_{HH} = 8.0 Hz), 0.64 (q, 2H, CH₂CH₃, ³J_{HH} = 8.2 Hz); ¹³C{¹H} NMR (100 MHz, THF-*d*₈) δ (ppm): 164.0 (C^{IV}), 155.7 (C^{IV}), 141.5 (C^{IV}), 140.8 (CH), 139.6 (C^{IV}), 131.0 (CH), 130.5 (C^{IV}), 129.2 (CH), 128.9 (CH), 128.4 (CH), 121.3 (CH), 115.1 (CH), 111.0 (CH), 12.8 (CH₂CH₃), 7.2 (CH₂CH₃); Anal. Calc. (ZnC₁₇H₁₅NO): C, 64.88%; H, 4.80%; N, 4.45%. Found: C, 64.75%; H, 4.82%; N, 4.50%.

Compound Zn-G. ¹H NMR (400 MHz, THF-*d*₈) δ (ppm): 8.48 (d, 1H, CH, ³J_{HH} = 8.6 Hz), 7.54 (d, 1H, CH, ³J_{HH} = 8.6 Hz), 7.49 (s, 1H, CH), 4.50 (t, 2H, (Cp(CH)C≡C), ³J_{HH} = 1.6 Hz), 4.24 (s, 5H, (Cp(CH))), 4.21 (t, 2H, (Cp(CH)C≡C), ³J_{HH} = 1.6 Hz), 2.83 (s, 3H, CH₃), 1.33 (t, 3H, CH₂CH₃, ³J_{HH} = 8.1 Hz), 0.44 (q, 2H, CH₂CH₃, ³J_{HH} = 8.1 Hz); ¹³C{¹H} NMR (125.3 MHz, THF-*d*₈) δ (ppm): 165.5 (C^{IV}), 157.2 (C^{IV}), 141.5 (C^{IV}), 137.1 (CH), 132.5 (CH), 126.2 (C^{IV}), 124.0 (CH), 112.1 (C^{IV}), 109.9 (C^{IV}), 93.2 (C≡C), 85.2 (C≡C), 72.2 (Cp(CH)C≡C), 70.9 (Cp(CH)), 69.4 (Cp(CH)C≡C), 68.1 (Cp(C^{IV})C≡C), 24.8 (CH₃), 13.6 (CH₂CH₃), -1.3 (CH₂CH₃); Anal. Calc. (ZnC₂₄H₂₀ClFeNO): C, 58.22%; H, 4.07%; N, 2.83%. Found: C, 58.33%; H, 4.12%; N, 2.91%.

Acknowledgements

The research was supported by funding from the EPSRC (EP/K035274/1, EP/K014070/1). CB acknowledges an EPSRC Doctoral Prize Fellowship for financial support. DWB acknowledges the Imperial-UBC Summer Research Placement Exchange 2014 for financial support. Purac Plc. are thanked for the donation of *rac*-lactide.

References

- (a) P. J. Dijkstra, H. Z. Du and J. Feijen, *Polym. Chem.*, 2011, 2, 520–527; (b) J.-C. Buffet and J. Okuda, *Polym. Chem.*, 2011, 2, 2758–2763; (c) N. Ajellal, J. F. Carpentier, C. Guillaume, S. M. Guillaume, M. Helou, V. Poirier,



- Y. Sarazin and A. Trifonov, *Dalton Trans.*, 2010, **39**, 8363–8376; (d) R. H. Platel, L. M. Hodgson and C. K. Williams, *Polym. Rev.*, 2008, **48**, 11–63; (e) A. Arbaoui and C. Redshaw, *Polym. Chem.*, 2010, **1**, 801–826.
- 2 M. J. L. Tschan, E. Brule, P. Haquette and C. M. Thomas, *Polym. Chem.*, 2012, **3**, 836–851.
- 3 (a) A. Kowalski, A. Duda and S. Penczek, *Macromolecules*, 1998, **31**, 2114; (b) H. Du, A. H. Velders, P. J. Dijkstra, J. Sun, Z. Zhong, X. Chen and J. Feijen, *Chem. – Eur. J.*, 2009, **15**, 9836–9845; (c) Z. Y. Zhong, P. J. Dijkstra and J. Feijen, *Angew. Chem., Int. Ed.*, 2002, **41**, 4510–4513; (d) M. Normand, V. Dorcet, E. Kirillov and J. F. Carpentier, *Organometallics*, 2013, **32**, 1694–1709; (e) M. Bouyahyi, T. Roisnel and J.-F. Carpentier, *Organometallics*, 2011, **31**, 1458–1466; (f) M. Bouyahyi, T. Roisnel and J.-F. Carpentier, *Organometallics*, 2009, **29**, 491–500; (g) M. Bouyahyi, E. Grunova, N. Marquet, E. Kirillov, C. M. Thomas, T. Roisnel and J. F. Carpentier, *Organometallics*, 2008, **27**, 5815–5825; (h) T. M. Ovitt and G. W. Coates, *J. Am. Chem. Soc.*, 2002, **124**, 1316; (i) P. Hormnirun, E. L. Marshall, V. C. Gibson, A. J. P. White and D. J. Williams, *J. Am. Chem. Soc.*, 2004, **126**, 2688–2689; (j) D. J. Darensbourg and O. Karroonnirun, *Organometallics*, 2010, **29**, 5627–5634.
- 4 (a) X. Y. Wang, K. R. Liao, D. P. Quan and Q. Wu, *Macromolecules*, 2005, **38**, 4611–4617; (b) B. J. O'Keefe, L. E. Breyfogle, M. A. Hillmyer and W. B. Tolman, *J. Am. Chem. Soc.*, 2002, **124**, 4384–4393; (c) M. Stolt and A. Sodergard, *Macromolecules*, 1999, **32**, 6412–6417; (d) A. B. Biernesser, B. Li and J. A. Byers, *J. Am. Chem. Soc.*, 2013, **135**, 16553–16560.
- 5 (a) M. H. Chisholm, J. C. Gallucci and K. Phomphrai, *Inorg. Chem.*, 2004, **43**, 6717–6725; (b) M. H. Chisholm, J. Gallucci and K. Phomphrai, *Chem. Commun.*, 2003, 48–49; (c) M. Lamberti, A. Botta and M. Mazzeo, *Appl. Organomet. Chem.*, 2014, **28**, 140–145; (d) W. Yi and H. Ma, *Inorg. Chem.*, 2013, **52**, 11821–11835; (e) B. Liu, T. Roisnel, L. Maron, J.-F. Carpentier and Y. Sarazin, *Chem. – Eur. J.*, 2013, **19**, 3986–3994; (f) M.-W. Hsiao and C.-C. Lin, *Dalton Trans.*, 2013, **42**, 2041–2051; (g) L. Clark, G. B. Deacon, C. M. Forsyth, P. C. Junk, P. Mountford, J. P. Townley and J. Wang, *Dalton Trans.*, 2013, **42**, 9294–9312; (h) B. Liu, T. Roisnel, J.-P. Guegan, J.-F. Carpentier and Y. Sarazin, *Chem. – Eur. J.*, 2012, **18**, 6289–6301; (i) J. P. Davin, J.-C. Buffet, T. P. Spaniol and J. Okuda, *Dalton Trans.*, 2012, **41**, 12612–12618; (j) M. G. Cushion and P. Mountford, *Chem. Commun.*, 2011, **47**, 2276–2278; (k) J.-C. Buffet, J. P. Davin, T. P. Spaniol and J. Okuda, *New J. Chem.*, 2011, **35**, 2253–2257; (l) Z. Y. Zhong, M. J. K. Ankone, P. J. Dijkstra, C. Birg, M. Westerhausen and J. Feijen, *Polym. Bull.*, 2001, **46**, 51–57.
- 6 (a) M. J. Walton, S. J. Lancaster and C. Redshaw, *ChemCatChem*, 2014, **6**, 1892–1898; (b) H. Wang, Y. Yang and H. Ma, *Macromolecules*, 2014, **47**, 7750–7764; (c) F. Drouin, T. J. J. Whitehorne and F. Schaper, *Dalton Trans.*, 2011, **40**, 1396–1400; (d) M. H. Chisholm, J. C. Gallucci and K. Phomphrai, *Inorg. Chem.*, 2005, **44**, 8004–8010; (e) B. M. Chamberlain, M. Cheng, D. R. Moore, T. M. Ovitt, E. B. Lobkovsky and G. W. Coates, *J. Am. Chem. Soc.*, 2001, **123**, 3229–3238; (f) M. H. Chisholm, J. Gallucci and K. Phomphrai, *Inorg. Chem.*, 2002, **41**, 2785–2794; (g) V. Poirier, T. Roisnel, J.-F. Carpentier and Y. Sarazin, *Dalton Trans.*, 2009, 9820–9827; (h) J. C. Wu, B. H. Huang, M. L. Hsueh, S. L. Lai and C. C. Lin, *Polymer*, 2005, **46**, 9784–9792; (i) W.-C. Hung and C.-C. Lin, *Inorg. Chem.*, 2009, **48**, 728–734; (j) L. Wang and H. Ma, *Macromolecules*, 2010, **43**, 6535–6537; (k) T. J. J. Whitehorne, B. Vabre and F. Schaper, *Dalton Trans.*, 2014, **43**, 6339–6352; (l) C. Gallegos, V. Tabernero, F. M. Garcia-Valle, M. E. G. Mosquera, T. Cuenca and J. Cano, *Organometallics*, 2013, **32**, 6624–6627.
- 7 (a) J. Zhang, J. Xiong, Y. Sun, N. Tang and J. Wu, *Macromolecules*, 2014, **47**, 7789–7796; (b) L. N. Saunders, L. N. Dawe and C. M. Kozak, *J. Organomet. Chem.*, 2014, **749**, 34–40; (c) B. Calvo, M. G. Davidson and D. Garcia-Vivo, *Inorg. Chem.*, 2011, **50**, 3589–3595; (d) Y. Huang, Y.-H. Tsai, W.-C. Hung, C.-S. Lin, W. Wang, J.-H. Huang, S. Dutta and C.-C. Lin, *Inorg. Chem.*, 2010, **49**, 9416–9425.
- 8 (a) Y. Huang, W. Wang, C.-C. Lin, M. P. Blake, L. Clark, A. D. Schwarz and P. Mountford, *Dalton Trans.*, 2013, **42**, 9313–9324; (b) Y. Lemmouchi, M. C. Perry, A. J. Amass, K. Chakraborty and E. Schacht, *J. Polym. Sci., Part A: Polym. Chem.*, 2008, **46**, 5348–5362; (c) L. Sipos and M. Zsuga, *J. Macromol. Sci., Part A: Pure Appl. Chem.*, 1997, **34**, 1269–1284; (d) Z. Jedlinski, P. Kurcok and R. W. Lenz, *J. Macromol. Sci., Part A: Pure Appl. Chem.*, 1995, **32**, 797–810; (e) Z. Jedlinski, P. Kurcok, M. Kowalczyk, A. Matuszowicz, P. Dubois, R. Jerome and H. R. Kricheldorf, *Macromolecules*, 1995, **28**, 7276–7280; (f) H. R. Kricheldorf and C. Boettcher, *Makromol. Chem.*, 1993, **73**, 47–64.
- 9 (a) Y. Sarazin, R. H. Howard, D. L. Hughes, S. M. Humphrey and M. Bochmann, *Dalton Trans.*, 2006, 340–350; (b) Z. R. Turner, J.-C. Buffet and D. O'Hare, *Organometallics*, 2014, **33**, 3891–3903; (c) C. J. Chuck, M. G. Davidson, G. G. du Sart, P. K. Ivanova-Mitseva, G. I. Kociok-Koehn and L. B. Manton, *Inorg. Chem.*, 2013, **52**, 10804–10811; (d) A. Sauer, A. Kapelski, C. Fliedel, S. Dagorne, M. Kol and J. Okuda, *Dalton Trans.*, 2013, **42**, 9007–9023; (e) B. J. Jeffery, E. L. Whitelaw, D. Garcia-Vivo, J. A. Stewart, M. F. Mahon, M. G. Davidson and M. D. Jones, *Chem. Commun.*, 2011, **47**, 12328–12330; (f) J.-C. Buffet, A. N. Martin, M. Kol and J. Okuda, *Polym. Chem.*, 2011, **2**, 2378–2384; (g) C. K. A. Gregson, V. C. Gibson, N. J. Long, E. L. Marshall, P. J. Oxford and A. J. P. White, *J. Am. Chem. Soc.*, 2006, **128**, 7410–7411; (h) C. K. A. Gregson, I. J. Blackmore, V. C. Gibson, N. J. Long, E. L. Marshall and A. J. P. White, *Dalton Trans.*, 2006, 3134–3140; (i) S. Gendler, S. Segal, I. Goldberg, Z. Goldschmidt and M. Kol, *Inorg. Chem.*, 2006, **45**, 4783–4790; (j) A. J. Chmura, M. G. Davidson, M. D. Jones, M. D. Lunn, M. F. Mahon, A. F. Johnson, P. Khunkamchoo, S. L. Roberts and S. S. F. Wong, *Macromolecules*, 2006, **39**,



- 7250–7257; (k) Y. Kim, G. K. Jnaneshwara and J. G. Verkade, *Inorg. Chem.*, 2003, **42**, 1437–1447.
- 10 (a) C. Bakewell, A. J. P. White, N. J. Long and C. K. Williams, *Inorg. Chem.*, 2013, **52**, 12561–12567; (b) C. Bakewell, R. H. Platel, S. K. Cary, S. M. Hubbard, J. M. Roaf, A. C. Levine, A. J. P. White, N. J. Long, M. Haaf and C. K. Williams, *Organometallics*, 2012, **31**, 4729–4736; (c) K. Sokołowski, I. Justyniak, W. Śliwiński, K. Sołtys, A. Tulewicz, A. Kornowicz, R. Moszyński, J. Lipkowski and J. Lewiński, *Chem. – Eur. J.*, 2012, **18**, 5637–5645; (d) W. Zhang, S. Liu, W. Yang, X. Hao, R. Glaser and W. H. Sun, *Organometallics*, 2012, **31**, 8178–8188; (e) B. Kamenar, C. K. Prout and J. D. Wright, *J. Chem. Soc.*, 1965, 4851–4867; (f) M. Pasquali, P. Fiaschi, C. Floriani and P. F. Zanazzi, *J. Chem. Soc., Chem. Commun.*, 1983, 613–614; (g) W.-H. Sun, M. Shen, W. Zhang, W. Huang, S. Liu and C. Redshaw, *Dalton Trans.*, 2011, **40**, 2645–2653.
- 11 G. Delapierre, J. M. Brunel, T. Constantieux and G. Buono, *Tetrahedron: Asymmetry*, 2001, **12**, 1345–1352.
- 12 (a) Y. Fazaeli, M. M. Amini and S. W. Ng, *Acta Crystallogr., Sect. E: Struct. Rep. Online*, 2008, **64**, m1509–m1509; (b) M. Mirzaee and M. M. Amini, *Appl. Organomet. Chem.*, 2005, **19**, 339–342; (c) Y. Fazaeli, E. Najafi, M. M. Amini and S. W. Ng, *Acta Crystallogr., Sect. E: Struct. Rep. Online*, 2009, **65**, m271–m271; (d) P. H. Bird, A. R. Fraser and C. F. Lau, *Inorg. Chem.*, 1973, **12**, 1322–1328; (e) W. F. Zeng, Y. S. Chen, M. Y. Chiang, S. S. Chern and C. P. Cheng, *Polyhedron*, 2002, **21**, 1081–1087; (f) F. Grasset, J.-B. Cazaux, L. Magna, P. Braunstein and H. Oliver-Bourbigou, *Dalton Trans.*, 2012, **41**, 10396–10404.
- 13 K. Sokołowski, I. Justyniak, W. Śliwiński, K. Sołtys, A. Tulewicz, A. Kornowicz, R. Moszyński, J. Lipkowski and J. Lewiński, *Chem. – Eur. J.*, 2012, **18**, 5637–5645.
- 14 K. L. Orchard, J. E. Harris, A. J. P. White, M. S. P. Shaffer and C. K. Williams, *Organometallics*, 2011, **30**, 2223–2229.
- 15 (a) X. Wang, A. Thevenon, J. L. Brosmer, I. Yu, S. I. Khan, P. Mehrkhodavandi and P. L. Diaconescu, *J. Am. Chem. Soc.*, 2014, **136**, 11264–11267; (b) E. M. Broderick, P. S. Thuy-Boun, N. Guo, C. S. Vogel, J. Sutter, J. T. Miller, K. Meyer and P. L. Diaconescu, *Inorg. Chem.*, 2011, **50**, 2870–2877; (c) E. M. Broderick, N. Guo, C. S. Vogel, C. L. Xu, J. Sutter, J. T. Miller, K. Meyer, P. Mehrkhodavandi and P. L. Diaconescu, *J. Am. Chem. Soc.*, 2011, **133**, 9278–9281.
- 16 J. Coudane, C. Ustariz-Peyret, G. Schwach and M. Vert, *J. Polym. Sci., Part A: Polym. Chem.*, 1997, **35**, 1651–1658.
- 17 (a) E. L. Whitelaw, M. D. Jones and M. F. Mahon, *Inorg. Chem.*, 2010, **49**, 7176–7181; (b) K.-C. Hsieh, W.-Y. Lee, L.-F. Hsueh, H. M. Lee and J.-H. Huang, *Eur. J. Inorg. Chem.*, 2006, **2006**, 2306–2312; (c) M. Hu, M. Wang, H. Zhu, L. Zhang, H. Zhang and L. Sun, *Dalton Trans.*, 2010, **39**, 4440–4446.
- 18 (a) S. K. Russell, C. L. Gamble, K. J. Gibbins, K. C. S. Juhl, W. S. Mitchell, A. J. Tumas and G. E. Hofmeister, *Macromolecules*, 2005, **38**, 10336–10340; (b) A. J. Chmura, M. G. Davidson, C. J. Frankis, M. D. Jones and M. D. Lunn, *Chem. Commun.*, 2008, 1293–1295; (c) A. Stopper, J. Okuda and M. Kol, *Macromolecules*, 2012, **45**, 698–704; (d) J.-C. Buffet and J. Okuda, *Chem. Commun.*, 2011, **47**, 4796–4798.
- 19 J. A. Dean, *Lange's Handbook of Chemistry*, McGraw-Hill Inc., 1999.
- 20 (a) M. H. Chisholm, J. C. Gallucci, H. Zhen and J. C. Huffman, *Inorg. Chem.*, 2001, **40**, 5051–5054; (b) M. P. Coles and P. B. Hitchcock, *Eur. J. Inorg. Chem.*, 2004, **2004**, 2662–2672.
- 21 C. C. Roberts, B. R. Barnett, D. B. Green and J. M. Fritsch, *Organometallics*, 2012, **31**, 4133–4141.
- 22 (a) H. Y. Chen, H. Y. Tang and C. C. Lin, *Macromolecules*, 2006, **39**, 3745–3752; (b) C. K. Williams, L. E. Breyfogle, S. K. Choi, W. Nam, V. G. Young, M. A. Hillmyer and W. B. Tolman, *J. Am. Chem. Soc.*, 2003, **125**, 11350–11359.
- 23 (a) R. H. Platel, A. J. P. White and C. K. Williams, *Chem. Commun.*, 2009, 4115–4117; (b) N. Ajellal, J. F. Carpentier, C. Guillaume, S. M. Guillaume, M. Helou, V. Poirier, Y. Sarazin and A. Trifonov, *Dalton Trans.*, 2010, **39**, 8363–8376; (c) M. Bouyahyi, N. Ajellal, E. Kirillov, C. M. Thomas and J. F. Carpentier, *Chem. – Eur. J.*, 2011, **17**, 1872–1883; (d) K. Nie, L. Fang, Y. Yao, Y. Zhang, Q. Shen and Y. Wang, *Inorg. Chem.*, 2012, **51**, 11133–11143; (e) H. Ma, T. P. Spaniol and J. Okuda, *Angew. Chem., Int. Ed.*, 2006, **45**, 7818–7821.
- 24 M. H. Chisholm, K. Choojun, A. S. Chow and G. Fraenkel, *Angew. Chem., Int. Ed.*, 2013, **52**, 3264–3266.

